Electrochemical Preparation of Pyronin Y Thin Films on Gold Substrates

Murat Alanyalıoğlu, Mustafa Arık

Department of Chemistry, Arts and Sciences Faculty, Atatürk University, 25240 Erzurum, Turkey

Received 2 March 2008; accepted 7 July 2008
DOI 10.1002/app.29038
Published online 26 September 2008 in Wiley InterScience (www.interscience.wiley.com).

ABSTRACT: Cyclic voltammetry, chronoamperometry, UV-vis absorption spectroscopy, fluorescence spectroscopy, FTIR spectroscopy, and AFM techniques have been employed to investigate pyronin Y thin films formed on Au(111) substrates by electrochemical oxidation of pyronin Y monomer. The medium used in the electropolymerization was an anhydrous acetonitrile solution containing 0.1*M* $TBAClO_4$ as supporting electrolyte. Anodic electropolymerization potential (1450 mV) of pyronin Y has been obtained from cyclic voltammetry data. Solid-state electropolymerization of pyronin Y was performed by the potential-controlled electrolysis technique. Chronoamperometry studies indicate that the adsorption of pyronin Y takes place in an instantaneous three-dimensional nucleation and growth mechanism which is accompanied by random adsorption. UV-vis absorption and fluorescence spectra of the electrolysis solution as a function of electrodeposition time show the adsorption of insoluble pyronin Y films on Au electrode surface. FTIR-specular reflectance of a polymer coated Au electrode reveals that there is a possible C—C coupling in the formation of polymeric pyronin Y structure. A well ordered polymeric chain structure of pyronin Y on Au(111) has been observed from AFM data. © 2008 Wiley Periodicals, Inc. J Appl Polym Sci 111: 94–100, 2009

Key words: electrochemistry; solid-state polymerization; dyes; nucleation; AFM

INTRODUCTION

Xanthene dyes such as pyronin Y have high absorption coefficients and are easily processed and can be functionalized to obtain the specific optical and electrical properties. Owing to these properties, xanthene dyes are widely used, especially for dye lasers,[1] solar energy conversion devices,[2] photosensitizer compounds for chemical reactions,[3] and nonlinear optical media for many applications.[4] The molecular system of pyronin Y exhibits the phenomenon of extended conjugation, which is in fact responsible for its absorption in the longer wavelength of visible spectrum. Two electronic structures of pyronin Y are possible in which the conjugation is totally different, one where the oxygen assumes positive charge and in other possible structure, the nitrogen assumes positive charge. However, because the nitrogen is less electronegative than oxygen, the structure with positive nitrogen is more likely one.[5] The chemical structure of pyronin Y is given in Scheme 1.

Many theoretical models[6–8] have been proposed to describe the relationship between physical properties and the molecular packing within aggregates both in solution and at surfaces. It is known that the molecular orientations in the unit cell affect the excitonic transitions.[9] The observation that substrates modified with dye polymer films show excellent catalytic and photoelectrochemical properties has stimulated much recent activity in characterizing sensitized redox reactions in nonhomogenous media. Therefore, new strategies have aimed at tailoring only the surface of materials or a thin-surface layer while preserving the bulk properties of the underlying support.[10] Electropolymerization is one of the most important techniques for obtaining oligomer and polymer thin films. Electrochemical polymerization arises from the oxidation of monomer to its radical cation followed by the coupling of these radicals to produce a hydro-dimer dication, which leads to a dimer after the loss of two protons and rearomatization. The electrochemical polymerization mechanism of pyronin Y presents many similarities with the electrooxidation of some xanthene dye compounds. Electrochemical behavior of pyronin B,[11] xanthene,[12] and other xanthene derivatives[13] have been studied. However, electrochemical behavior and electropolymerization of pyronin Y have not been studied until now.

The main purpose of this article is to investigate the electrooxidation behavior of pyronin Y as well as the possibility of forming a new class of polymeric

Correspondence to: M. Alanyalıoğlu.
Contract grant sponsor: Atatürk University.

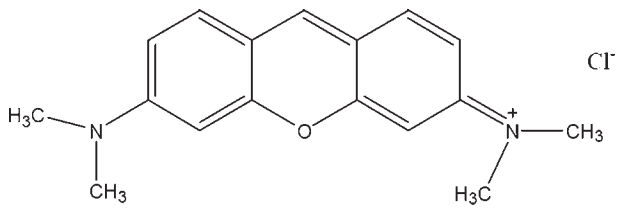

Scheme 1 Chemical structure of pyronin Y.

structure on Au(111) single crystal electrode. Cyclic voltammetry, chronoamperometry, UV-vis absorption, fluorescence, FTIR-specular reflectance, and AFM results showed that polymeric films of pyronin Y can be synthesized on Au substrates.

EXPERIMENTAL

Materials

Pyronin Y was purchased from Sigma. Acetonitrile (Fluka Chemika) was used as solvent. Acetonitrile was purified by drying with calcium hydride, followed by distillation over phosphorus pentoxide, and then it was kept under molecular sieves (3A Merck) to eliminate its water content as much as possible. Tetrabutylammonium perchlorate, TBA-ClO_4 (Fluka Chemika) was used as supporting electrolyte in electrochemical cell. Pyronin Y solution was stored in the dark as concentrated stock solutions of $1.0 \times 10^{-3}M$ in acetonitrile. In all experiments, pyronin Y solutions of $1.0 \times 10^{-5}M$ in acetonitrile were prepared by diluting the stock solution to avoid self-absorption effect.

Electrochemistry

All electrochemical experiments were performed with an Epsilon electrochemical analyzer system connected to a three electrode cell at room temperature. AFM experiments were applied on Au(111) single crystal substrates that were prepared as previously described.[14] Polycrystalline Au electrodes contain a few large (111) facets that are visible by eye. Dimensions of these facets are $\sim$ 1000 μm. Prior to each electrochemical experiment, the electrode was flame-annealed in H_2-O_2 flame for about 30 s, and after a short time cooling in air, the electrode was quenched in Milli-Q water. This procedure was repeated at least five times. An indium tin oxide (ITO)-coated glass electrode (Delta Technologies) with sheet resistance of 10 Ω cm^{-2} was also used as working electrode. ITO-coated glass electrode was cleaned by sonication in detergent solution for 5 min and then rinsed with a large amount of doubly distilled water. Further sonication in ethanol for 5 min was applied before being blown dry with a stream nitrogen. Gold foil (0.1-mm thick, Alfa Aesar) working electrodes were used for FTIR-specular reflectance experiments. In all cases, an Ag/AgCl (3*M* NaCl) (Bioanalytical Systems, West Lafayette, IN) electrode served as reference electrode, and a Pt wire electrode was used as counter electrode. The solutions were deoxygenated by passing dry nitrogen through the electrochemical cell for 30 min prior to each experiment.

Instrumentation

Ex-situ scanning tunneling microscopy (STM) and atomic force microscopy (AFM) measurements were performed in ambient conditions, with a molecular imaging model PicoScan instrument. Pt-Ir wires (90 : 10) were used as tunneling tips for STM imaging. All AFM images were acquired in noncontact mode using silicon probes (Pointprobe) having resonance frequency of 190 kHz and force constant of 48*N*/m. *Ex-situ*-FTIR absorbance (KBr) and specular reflectance spectra were obtained with a spectrum one model Perkin–Elmer FTIR instrument. UV-vis absorption and fluorescence spectra of samples were taken with a Shimadzu UV-3101PC UV-vis-NIR spectrophotometer and a Shimadzu RF-5301PC spectrofluorophotometer, respectively.

RESULTS AND DISCUSSION

Cyclic voltammetry

The anodic oxidation of pyronin Y was performed in anhydrous acetonitrile solution containing 0.1*M* $TBAClO_4$ on Au electrodes. The cyclic voltammograms without and with $1.0 \times 10^{-5}M$ pyronin Y are shown in Figure 1(a,b), respectively. The positive scan shows an oxidation peak at $\sim$ 1430 mV (peak I) corresponding to the oxidation of pyronin Y monomer [Fig. 1(b)]. Reversing the potential, a well-defined reductive peak is observed at 1160 mV (peak II). The peak potential separation ΔE_p, for peak I and II is about 270 mV. Thus, these peaks are not characteristic of Nernstian redox couples. It can be deduced that the peak II corresponds to the reduction of electrodeposited pyronin Y thin films. We have also performed this voltammetric experiment by using ITO-coated glass substrates as a working electrode. High surface resistance of ITO-coated glass electrode did not give us an opportunity to work, and no peaks for oxidation or reduction of pyronin Y monomer were observed.

To confirm the existence of PyY films on gold electrode surface, a polymeric film was formed on the electrode surface by keeping the potential of the Au working electrode constant at 1450 mV for 15 min in

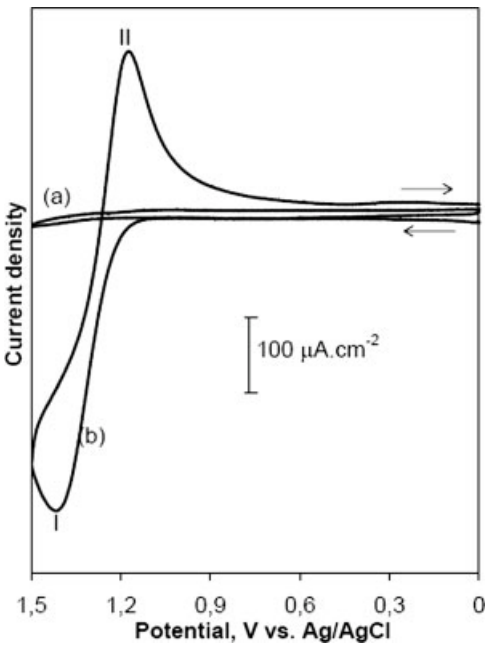

Figure 1 Cyclic voltammetry of polycrystalline Au electrode in acetonitrile solution of (a) 0.1*M* $TBAClO_4$, (b) $1.0 \times 10^{-5}M$ pyronin Y + 0.1*M* $TBAClO_4$. Scan rate: 100 mV s^{-1}.

acetonitrile solution containing 0.1*M* $TBAClO_4$, and $1.0 \times 10^{-5}M$ pyronin Y. It was removed from electrochemical cell and washed thoroughly with acetonitrile solution. After this process, voltammetric behavior of polymer-coated Au electrode against the $Fe[(CN)_6]^{-3}$/ $Fe[(CN)_6]^{-4}$ redox system was studied. Neither anodic nor cathodic peaks associated with redox system were obtained. This result reveals the existence of a polymeric film on the electrode surface. Salah and Mhalla[12] have studied anodic oxidation of xanthene molecule on platinum disk electrode in acetonitrile solution and proposed an ECE type oxidation. As a guide to this reference and our experiments, the following mechanism for the oxidative electrode reaction can be proposed.

$$PyY \rightarrow PyY^{\cdot +} + e^- \quad (1)$$

$$PyY^{\cdot +} \xrightarrow[PyY \text{ or } PyY^{\cdot +}]{-H^+} PyY - PyY \rightarrow \text{Oligomer or polymer} \quad (2)$$

Chronoamperometry

Chronoamperometry experiments were applied to investigate the nucleation and growth mechanism of pyronin Y. Typical current density-time transient for the electrooxidation of pyronin Y at 1450 mV from the acetonitrile solution containing $1.0 \times 10^{-5}M$ pyronin Y and 0.1*M* $TBAClO_4$ on Au electrode is presented in Figure 2. From A to B, the current density rises as monomer oxidation and polymer nucleation occurs. Current density reaches a maximum at about 3.5 s (Point B). Between B and C, current density declines gradually because of three-dimensional nucleation for a diffusion-limited process. In this section, the coalescence of nuclei is supposed to occur. Point C is attributed to the starting point of the actual film deposition.[15] After point C, current density keeps almost constant. The same behavior has been obtained for electropolymerization of pyrrole,[16,17] aniline or aniline derivatives,[18,19] and thiophene or thiophene derivatives.[15,20,21] However, this type of current density-time transient is quite common for two-dimensional nucleation and growth. The conducting polymer films of interest are made purposely much thicker than a mono-molecular layer. Therefore, the deposition of polymer films occurs in three-dimensions. According to Li and Albery,[20] two possible mechanisms are possible for polymer films: Progressive two-dimensional layer-by-layer nucleation and instantaneous three-dimensional nucleation and growth.

Experimental current density-time transient data consist of two different terms, a random adsorption term and a nucleation and growth term. As given by the following equation:

$$J_{\text{total}} = J_{\text{nucleation}} + J_{\text{random}} \quad (3)$$

The current density for random adsorption term is

$$J_{\text{random}} = k \exp(-k't) \quad (4)$$

In this process, current density is related to the empty surface area, molecules are adsorbed on the Au surface wherever it is empty. Therefore, current starts from a maximum and decays to zero, exponentially. Nucleation and growth term can be

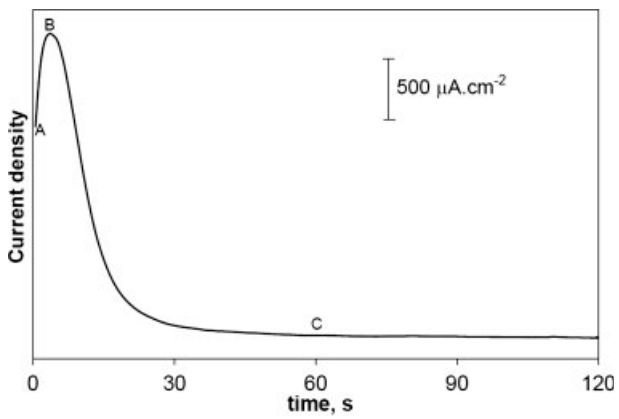

Figure 2 Current density-time transient obtained after electrooxidation of pyronin Y at 1450 mV from the acetonitrile solution containing $1.0 \times 10^{-5}M$ pyronin Y and 0.1*M* $TBAClO_4$ on polycrystalline Au substrate.

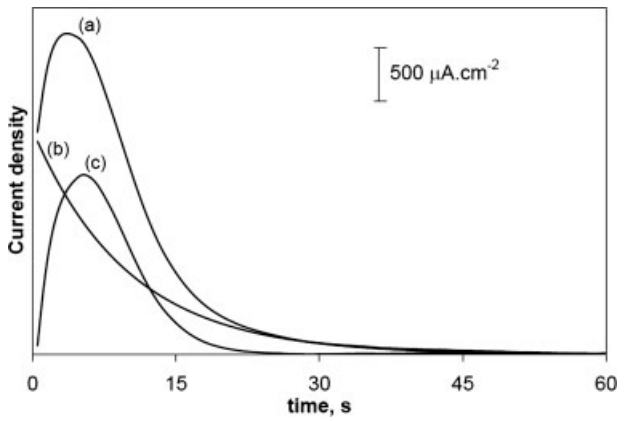

Figure 3 (a) Experimental current density-time transient (b) numerical fit of the random adsorption (c) and nucleation model.

described as either instantaneous or progressive. The current densities for these two cases are

$$J_{\text{ins}} = at\exp(-bt^2) \tag{5}$$

for the instantaneous case and

$$J_{\text{prog}} = ct\exp(-dt^3) \tag{6}$$

for progressive case. Instantaneous nucleation corresponds to slow growth of nuclei on a less number of active sites, all activated at the same time. Progressive nucleation corresponds to fast growth of nuclei on many active sites, all activated during the course of electrochemical process. Hence, the size distribution for instantaneous nucleation is expected to be much narrower than for progressive nucleation. A fit of measured transient was attempted to separate the random adsorption from the nucleation process, with eq. (3) using least-squares fits and working with multidimensional Newton routines. Figure 3 shows excellent fit of the data obtained for random adsorption [Fig. 3(b)] and nucleation and growth process [Fig. 3(c)] take place simultaneously at difference surface site. It is known that surface defects such as monatomic steps, holes, etc. are preferred sites for adsorption.[22] Figure 3 also exhibits that 54% of the total current is due to the random and 46% is due to nucleation and growth process. A reduced variable plot of the measured quantities (j/j_m versus t/t_m) allows us to determine the growth mechanism.[23] Figure 4 shows the reduced variable plots for the nucleation and growth data that is given in Figure 3(c). Calculated transients for instantaneous and progressive nucleation are shown for a direct comparison with the experimental data. The reduced variable plot clearly indicates that the nucleation mechanism is instantaneous. According to current density-time transient experiments and reference,[20] electropolymerization of pyronin Y takes place in an instantaneous three-dimensional nucleation and growth mechanism, which is accompanied by random adsorption. The published articles concerning the deposition of conducting polymers have been dominated by a mechanism of three-dimensional, and often instantaneous, nucleation and growth.[16,17,24–26]

UV-vis absorption and fluorescence results

UV-vis absorption and fluorescence spectra of pyronin Y in the electrolysis solution as a function of the electrodeposition time are given in Figure 5(a,b), respectively. The main peak that belongs to monomer appears at 547 nm in UV-vis absorption and at 564 nm in fluorescence spectra with $1.0 \times 10^{-5}M$ pyronin Y. Bands at 510 nm in UV-vis absorption and at 527 nm in fluorescence spectra that appear on the vibronic shoulder of the monomer bands are indicative of H-aggregate formation, and the intensity of this band depends on the dye concentration.[27] As can be seen in Figure 5, the intensity of monomer band decreases with increasing electrodeposition time for both absorption and fluorescence spectra. During the electropolymerization of pyronin Y, color of the electrolysis solution changes from pink to transparent, while color of the polymer film alters from transparent to brown with time. Because new absorption or fluorescence bands do not appear for any other species in the electrolysis solution, it can be concluded that the electrode surface is covered with insoluble polymeric films of pyronin Y.

FTIR results

The FTIR-absorbance spectrum of pyronin Y monomer and FTIR-specular reflectance spectrum of the polymeric film produced by electrooxidation of pyronin Y in acetonitrile solution containing $1.0 \times$

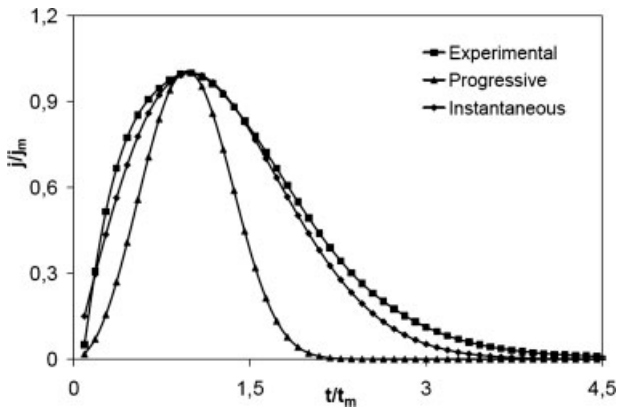

Figure 4 Recorded variable plots for the current density-time transient data shown in Figure 3(c).

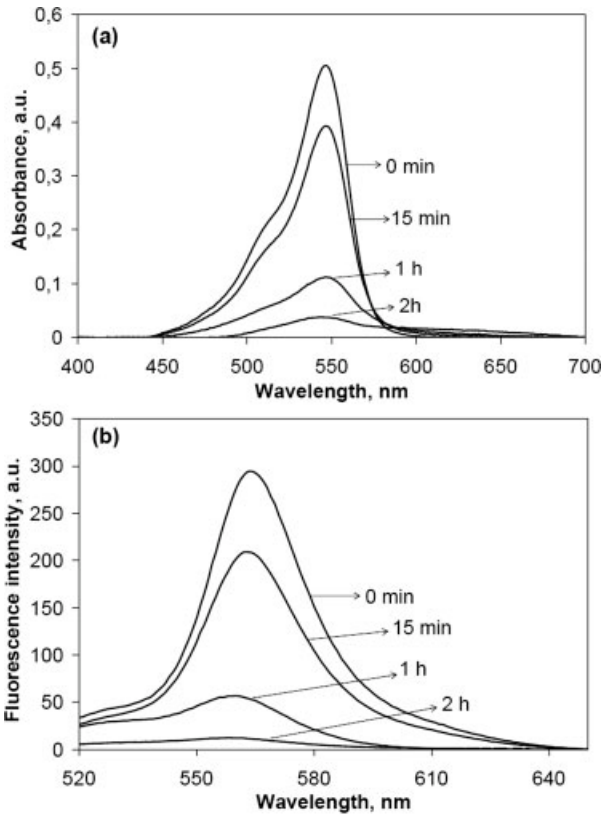

Figure 5 (a) UV-vis absorption, and (b) fluorescence spectra (excitaton λ: 480 nm) of electrolysis solution containing acetonitrile, 0.1*M* $TBAClO_4$, and $1.0 \times 10^{-5}M$ pyronin Y as a function of electrodeposition time.

$10^{-5}M$ pyronin Y and 0.1*M* $TBAClO_4$ at 1450 mV on Au-foil electrode are shown in Figure 6(a,b), respectively. Similar bands, characteristic of the pyronin Y monomer, are observed in both spectra: The strong bands in the region of 2800–3000 cm^{-1} can be associated with the aromatic C—H stretching vibration. The multiband absorptions of tertiary amine hydrochloride salts in the 2700–2330 cm^{-1} region are due to vibrations involving $^{+}N(CH_3)_2$ stretching. The bands at 2300–2400 cm^{-1} region can be attributed to the tertiary amine group. The vibrations involving CH_2 and CH_3 stretching (3000–2840 cm^{-1}) and bending modes (1470–1340 cm^{-1}) give rise to bands that are strong and characteristic in IR spectra. Bands in the 1340–1390 cm^{-1} region can be assigned to the CH_3 bending mode. Bands in the region of 1100–1180 cm^{-1} in the monomer IR spectrum can be associated with ether C—O symmetric and asymmetric stretching vibrations. In the polymer IR spectrum, the ether group overlaps with the band group at 920–1125 cm^{-1} region.[28]

On the other hand, some remarkable differences appear between these two IR spectra: Bands at 1100 and 625 cm^{-1} are characteristic of the ClO_4^- ion.[29] In the polymer spectrum, bands at 920–1125 cm^{-1} and 600–630 cm^{-1} region can be associated with ClO_4^- ion that diffuses into the polymer structure during the electropolymerization from the electrolysis solution that contains $TBAClO_4$. These bands do not appear in the pyronin Y monomer spectrum, which lacks the electrolyte. Many bands in the 1000–1600 cm^{-1} in-plane C—H bending vibration region interact (sometimes strongly) with various ring C—C vibrations.[28] In the monomer spectrum, peaks in the 1540–1620 cm^{-1} region can be attributed to C—H bending vibrations of aromatic rings. In the polymer spectrum, this band does not appear and a new band arises in the 1425–1500 cm^{-1} region. FTIR results indicate that there is a possible C—C coupling in the formation of polymeric pyronin Y structure. McNeill and Weiss[30] suggested that the xanthene polymerization occurs by C—C coupling.

AFM results

The film morphology was investigated by using STM and AFM. Because Au(111) substrate consists of atomically flat surface, we can use this flat surface as a reference surface for morphological studies. STM image of bare Au(111) is shown in Figure 7. Figure 8 shows the topographical noncontact mode AFM images representing the time evolution of pyronin Y thin film on an atomically flat Au(111) surface electrodeposited at 1450 mV for 1 min, 15 min, and 1 h, respectively. Z-height profiles of these images are also given under the images. The AFM image and z-height profile of pyronin Y film obtained for 1 min deposition [Fig. 8(a)] shows that the thin film is almost flat with a thickness of about 5 nm and the film consists of nuclei with 50 nm that group themselves into aggregates on the surface. This image obeys the chronoamperometry result that

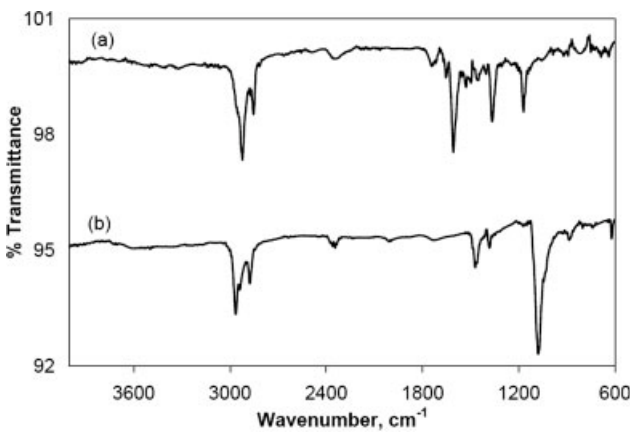

Figure 6 (a) FTIR-absorbance spectrum of pyronin Y monomer, and (b) FTIR-specular reflectance spectrum of the film produced by electrooxidation of $1.0 \times 10^{-5}M$ pyronin Y in acetonitrile and 0.1*M* $TBAClO_4$ solution at 1450 mV on Au-foil electrode.

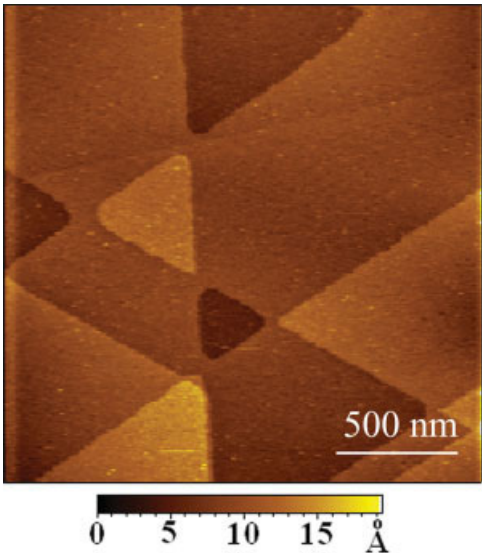

Figure 7 STM image of a bare Au(111) single crystal substrate. [Color figure can be viewed in the online issue, which is available at www.interscience.wiley.com]

is obtained at 1 min electrodeposition of pyronin Y. The AFM image and the z-height profile of pyronin Y film obtained after 15 min deposition [Fig. 8(b)] indicates a three-dimensional structure of the thickest polymeric film. Average grain size is 100 nm. It is an open structure where disordered packs of polymer probably arise from random adsorption, which occurs besides nucleation. The AFM image in Figure 8(c), recorded for a 1 h deposition time, reveals a surface containing well-ordered long chain features with almost uniform size of 150 nm. It can be deduced from this AFM image that instantaneous nucleation dominates the random adsorption by increasing the electrodeposition time, and strong intramolecular π-stacking forces cause preferential orientation of the oligomer or polymer chains in the film.[31]

CONCLUSIONS

We have shown here for first time that pyronin Y could be electropolymerized leading to a stable structure. UV-vis absorption and fluorescence spectra of electrolysis solution as a function of electrodeposition time exhibit the adsorption of insoluble pyronin Y deposits on the electrode surface. The reduced variable plot of the measured quantities (j/j_m versus t/t_m) obtained from current density-time transient results reveal that the electropolymerization of pyronin Y takes place in an instantaneous three-dimensional nucleation and growth mechanism, which is accompanied by random adsorption. Theoretical calculations indicate that 54% of the total current is due to the random adsorption and 46% is due to nucleation and growth process. The FTIR-

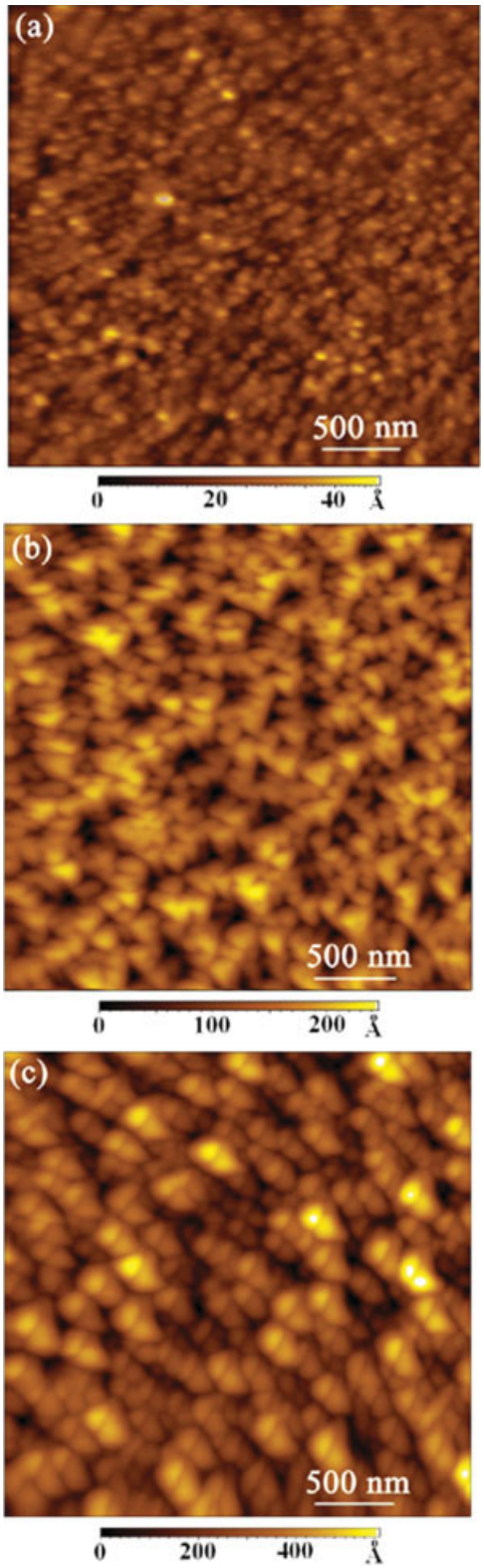

Figure 8 AFM images of pyronin Y films on Au(111) substrate electrodeposited at 1450 mV from acetonitrile solution containing $1.0 \times 10^{-5}M$ pyronin Y, and $0.1M$ $TBAClO_4$ for various times (a) 1 min, (b) 15 min, and (c) 1 h. [Color figure can be viewed in the online issue, which is available at www.interscience.wiley.com].

specular reflectance spectrum of the polymeric film shows bands characteristic of aromatic C—H deformation vibrations. This is an evidence for C—C coupling in the film formation. A well ordered polymeric chain structure of pyronin Y on Au(111) substrate is obtained from AFM data. Further investigations toward the electropolymerization of the other xanthene dyes such as pyronin B and florescein are in progress, which may result in a new class of materials for technological applications.

References

1. Drexhage, K. H. In Dye Lasers, 2nd ed.; Schaefer, F. P., Ed.; Spring: New York, 1977, p 143.
2. Misawa, H.; Sakuraki, H.; Usui, Y.; Tokumaru, K. Chem Lett 1983, 1021.
3. Gollnick, K.; Schenk, G. O. Pure Appl Chem 1964, 9, 507.
4. Kramer, M. A.; Tompkin, W. R.; Boyd, R. W. Phys Rev A 1986, 34, 2026.
5. Sharma, G. D.; Gupta, S. K.; Roy, M. S. Thin Solid Films 1998, 333, 176.
6. McRae, E. G.; Kahsa, M. J. J. Chem Phys 1958, 28, 721.
7. Kato, T.; Sasaki, S.; Abe, S.; Kobayashi, S. Chem Phys 1998, 230, 209.
8. Scherer, P. O. J.; Fisher, S. F. Chem Phys 1984, 86, 269.
9. Owens, R. W.; Smith, D. A. Langmuir 2000, 16, 562.
10. Zhong, A.; Lin, X.; Chen, D.; Zhou, Z. J Appl Polym Sci 2003, 87, 1029.
11. Sun, W.; You, J.; Hu, X; Jiao, K. Anal Lett 2006, 39, 33.
12. Salah, N. B.; Mhalla, F. M. J Electroanal Chem 2000, 485, 42.
13. Su, G-J.; Yin, S-X.; Wan, L-J.; Zhao, J-C.; Bai, C-L. Surf Sci 2004, 551, 204.
14. Hamelin, A. Mod Aspects Electrochem 1985, 16, 1.
15. Chao, F.; Costa, M.; Jin, G.; Tian, C. Electrochim Acta 1994, 39, 197.
16. Asavapiriyanont, S.; Chandler, G. K.; Gunawardena, G. A.; Pletcher, D. J Electroanal Chem 1984, 177, 245.
17. Miller, L. L.; Zinger, B.; Zhou, Q.-X. J Am Chem Soc 1987, 109, 2267.
18. Bade, K.; Tsakova, V.; Schultze, J. W. Electrochim Acta 1992, 37, 2255.
19. Cordova, R.; Valle, M. A. D.; Arratia, A.; Gomez, H.; Schrebler, R. J Electroanal Chem 1994, 377, 75.
20. Li, F.; Albery, W. J. Electrochim Acta 1992, 37, 393.
21. Skompska, M. Electrochim Acta 1998, 44, 357.
22. Alanyalıoğlu, M.; Çakal, H.; Öztürk, A. E.; Demir, Ü. J Phys Chem B 2001, 105, 10588.
23. Bewick, A.; Fleiscmann, M.; Thirsk, H. R. Trans Faraday Soc 1962, 58, 2200.
24. Hillman, A. R.; Mallen, E. F. J Electroanal Chem 1988, 243, 403.
25. Dian, G.; Merlet, N.; Barkey, G.; Outurquin, F.; Paulmier, C. J Electroanal Chem 1987, 238, 225.
26. Rubinstein, I.; Rishpon, J.; Sabatani, E.; Redondo, A.; Gottesfeld, S. J Am Chem Soc 1990, 112, 6135.
27. Arık, M.; Onganer, Y. Chem Phys Lett 2003, 375, 126.
28. Vien, D. L.; Colthup, N. L.; Fateley, W. G.; Grasselli, J. G. The Handbook of Infrared and Raman Characteristic Frequencies of Organic Molecules; Academic Press: California, 1991.
29. Tourilon, G.; Garner, F. J Electroanal Chem 1982, 135, 173.
30. McNeill, R.; Weiss, D. E. Aust J Chem 1959, 12, 643.
31. Ekinci, D.; Tümer, F.; Demir, Ü. Macromolecules 2004, 37, 7168.